LOCKIN-SPECKLE-INTERFEROMETRY WITH MODULATED OPTICAL AND INDUCTIVE EXCITATION

Philipp MENNER, Patrick SCHMITZ, Henry GERHARD, and Gerd BUSSE
INSTITUTE OF POLYMER-TECHNOLOGY, DEPARTMENT OF NON-DESTRUCTIVE TESTING (IKT-ZFP), UNIVERSITY OF STUTTGART,
Pfaffenwaldring 32, 70569 Stuttgart, Germany

Introduction

Speckle-interferometric methods like ESPI and shearography monitor the mechanical behaviour of an object under load, which makes them valuable tools for non-destructive testing. The load can be applied in various forms, like optical heating, pressure variation, mechanical loading etc. Lockin technique can improve classical speckle-interferometrical methods significantly by using a periodical loading and a Fourier transformation of the modulated object response. This paper discusses the general potential of this technique and presents the novel combination of Lockin speckle-interferometry and modulated inductive excitation.

Speckle Interferometry

Both Electronic Speckle Pattren Interferometry (ESPI) and shearography are well-known speckle-interferometric methods. The optical setups are shown in figure 1.

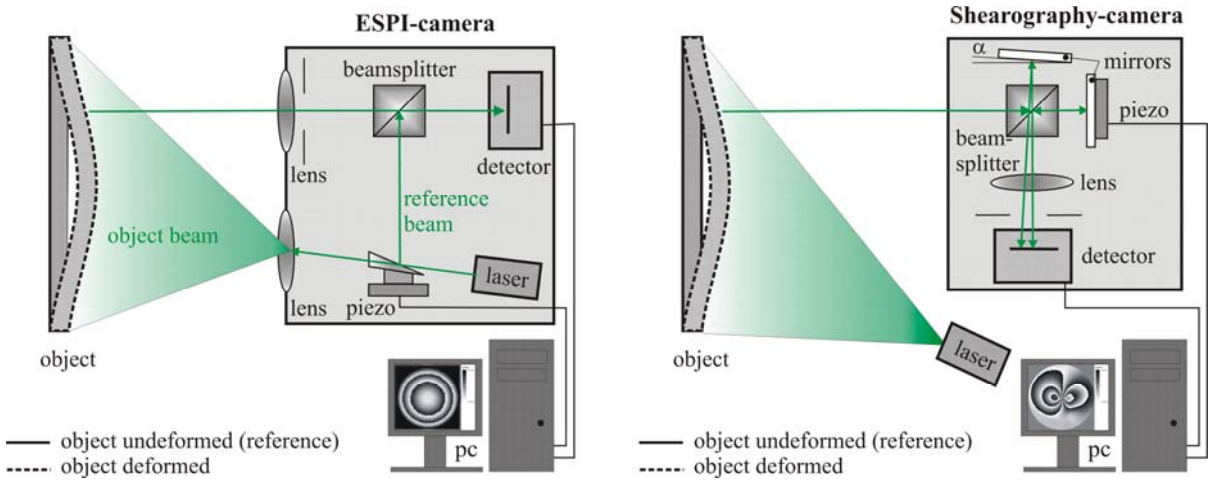

Figure 1: Setup of conventional ESPI (left) and conventional shearography (right).

Both methods are sensitive to very small displacement of objects by superposing the speckle patterns of two different object states. ESPI needs an internal reference beam to measure the absolute displacement of the object surface, while shearography is a self-referencing method which measures the gradient of the displacement in a certain ("shearing") direction [1]. The self-referencing reduces the sensitivity to external perturbations (e.g.vibrations), which makes the method more relevant for industrial use. Therefore we will focus on shearography, though the transfer of Lockin technique to speckle interferometry was done first on the ESPI method.

Conventionally, a static loading of the test object is used, i.e. optical heating, pressure variation, mechanical loading etc. After the load is applied, the measurement is started, and the displacement of the object is recorded as a sequence of fringe images (figure 2). Flaws change the displacement field locally and can therefore be detected. This is a very fast and simple

way to reveal mechanically relevant defects, but there are some drawbacks. Although many fringe images are recorded, only the one with the best contrast is evaluated, so most of the information is lost. Furthermore, the depth of defects cannot be determined, and sometimes the signal of a flaw is superposed by a large deformation of the sample itself which makes defect detection difficult.

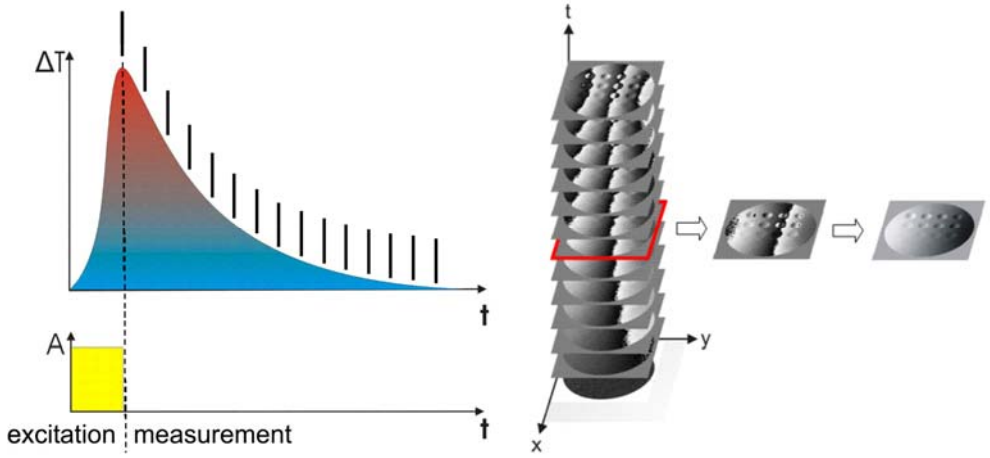

Figure 2: Conventional shearography measurement procedure: recording of image stack after static loading and evaluation of the best fringe image.

Lockin Speckle Interferometry

Optically excited Lockin shearography combines a conventional shearography sensor with dynamic excitation and a more complex data analysis. By intensity modulation of lamps, the object surface is heated periodically, thereby inducing a thermal wave in the object. At thermal boundaries, the wave is reflected back to the surface where it is superposed to the initial thermal wave. Thereby, both local phase angle and amplitude of the modulated temperature field are modified. The shearography sensor continuously monitors the periodical object displacement which is caused by the thermal wave. Like in conventional shearography, a sequence of fringe images is recorded, but not after a short, static excitation, but during a modulated excitation, and in contrast to the conventional method, not only one fringe image is evaluated, but the whole sequence of images ("image stack", figure 3).

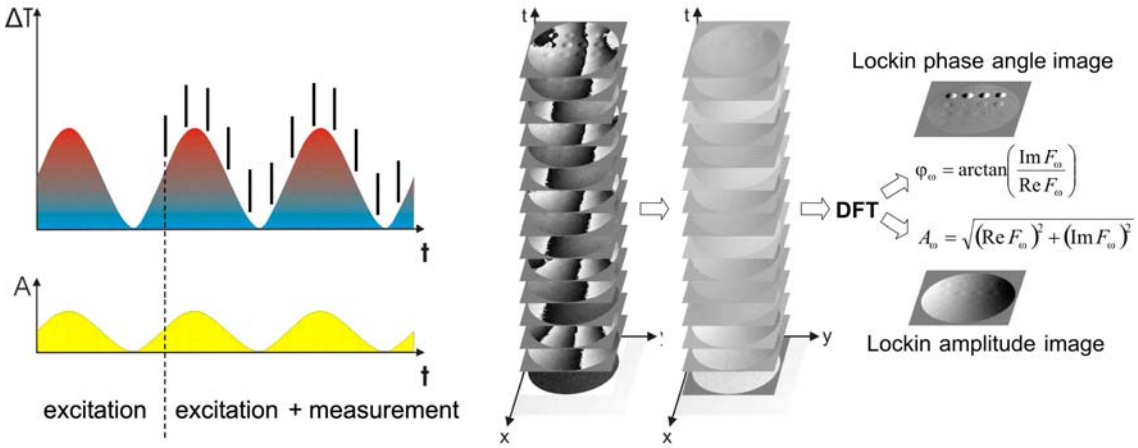

Figure 3: Lockin shearography measurement procedure: modulated object excitation with simultaneous displacement monitoring and image stack and data analysis.

After recording this image stack, a temporal phase unwrapping is performed. Then, a discrete Fourier transformation at the excitation frequency is applied to the signal of each pixel along

the time axis of the image stack. The discrete Fourier transformation extracts the phase and the amplitude of the sinusoidally modulated object displacement, therefore it condenses the image stack from up to 1000 images to only two images: the Lockin amplitude image (showing the local height of the modulation effect) and the Lockin phase image, displaying the local thermal phase delay between excitation and object response.

It is important to distinguish between optical phase images and thermal Lockin phase images: optical phase images are interferometric high-contrast fringe images which are obtained by temporal phase shifting, i.e. by systematical changes of optical path lengths and therewith the phase difference of two light waves. These are the images that the image stack consists of. The Lockin phase image, however, is the result of temporal analysis of the image stack, i.e. it shows the phase angle for each pixel, which corresponds to the local temporal delay between remotely injected modulated heat flow and object response. This principle of signal evaluation of an image stack is well known from optically excited Lockin Thermography [2,3,4] and could be transferred successfully to ESPI [2,5,6] and to shearography [7].

In an intact sample with constant thickness, all areas of the object are deforming with a constant temporal delay to the excitation, therefore the phase angle is constant all over the object. If there are changes in thickness, or if there is a damage (e.g. impact or delamination), this region is deforming periodically as well, but with a different temporal delay, caused by the reflection of the thermal wave.

Another advantage of Lockin shearography is also directly linked to the use of thermal waves. The thermal diffusion length μ_{th}, which is the depth where the amplitude of the thermal wave decreases to 1/e (about 37%), depends on excitation frequency [8]:

$$\mu_{th} = \sqrt{\frac{2\lambda}{\omega \cdot \rho \cdot c_p}} \tag{1}$$

with λ = thermal conductivity; ρ = density; c_p = specific heat capacity, and ω = modulation frequency of excitation.

The compression of the image stack to an amplitude image and a phase image via Fourier transformation corresponds to a weighted averaging. The signal-to-noise ratio is significantly improved by using not only one image for data evaluation, but a stack of up to 1000 fringe images.

Optical excitation is a fast and easy way to perform a non-contact excitation, but it has some limitations. It is difficult to deposit enough heat into objects with very bright or metallic surfaces, and the modulation frequencies are limited to 1Hz or less due to the thermal inertia of halogen lamps. Inductive heating does not only avoid these drawbacks, but it rather opens another promising kind of contrast mechanism.

The skin depth δ of the eddy current is:

$$\delta = \sqrt{\frac{2}{\omega \cdot \sigma \cdot \mu}} \tag{2}$$

with σ = electrical conductivity, μ = permeability and ω = resonance frequency of the oscillation circuit.

This means that in materials with a very high electrical conductivity (like aluminium) and therefore a small skin depth, a non-contact heating of the surface can be realised, regardless of the optical absorbtion coefficient. Furthermore, if a conductive surface is covered with an insulating material (e.g. an adhesion of polymer to metal), the inner boundary can be heated, and delaminations should be detected easily. In materials with low electrical conductivity and larger skin depth (like CFRP), not only the surface is heated, but the bulk material as well. Therefore, a reduced whole body displacement may be expected.

One the other hand, the excitation with eddy current is very inhomogeneous, and we found a strong influence of the material properties and the geometry of the test object and its orientation with respect to the inductor. Different types of CFRP are heated very differently, depending on the number of fibre-to-fibre contacts (at frequencies of 300kHz, purely resistive heating takes place). Samples made of CFRP fabric or several differently orientated layers of UD can be heated very well, while strictly unidirectional CFRP can hardly be excited.

Experimental Setup

For our Lockin shearography system (figure 4), we use a conventional self-made out-of-plane sensor head. The sample is illuminated by an array of laser diode modules that are mounted variably on four arms so that the object can be illuminated homogeneously, and the sensitivity vector is constant. For optical excitation, up to four lamps with filters can be used. Inductive excitation is realised by a water-cooled 1.5kW inductor. Effects due to convection of warm air are minimized by a steady air flow.

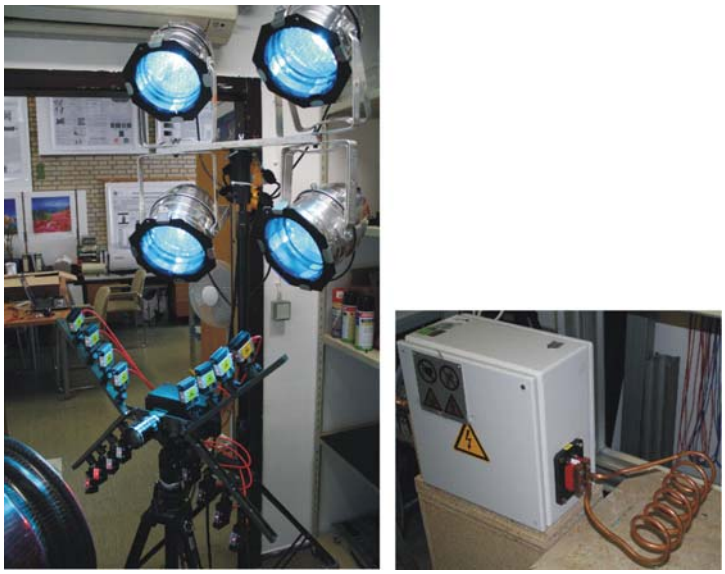

Figure 4: Experimental setup. Left: shearography sensor with red laser diode array on a tripod and halogen lamps with matching filters. Right: inductor for eddy current excitation.

Results

A blackened PMMA slab with two pairs of rows of flat bottom holes drilled from the rear side (remaining wall thickness 0.7mm and 1.4mm, respectively, figure 5, left) was measured with optically excited Lockin shearography. The demodulated conventional image with the best contrast of the sequence (figure 5, middle) displays the left pair of holes and barely the right pair while the Lockin phase image (figure 5, right) clearly shows both pairs. The SNR in the Lockin phase is about 10 times better than in the best image taken from the sequence. The significant improvement is based on the phase analysis of the frequency coded effect which is performed by dynamic excitation and the Fourier analysis.

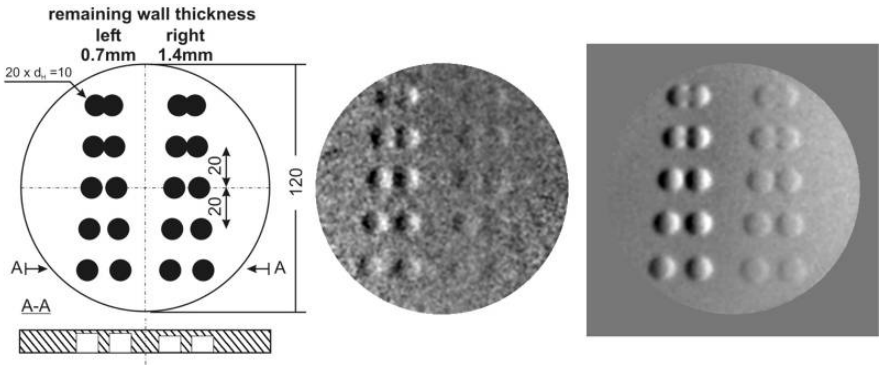

Figure 5: Left: scheme of PMMA sample. Middle: best image of image stack. Right: Lockin phase image derived from stack of images (excitation frequency 0.04Hz).

A 2mm thick PMMA plate was glued to an aluminium plate with equal thickness, with a small central area of missing adhesive. This simulated defect could be observed with conventional induction excited shearography, but it can be revealed much more clearly with induction excited Lockin shearography because of the significantly enhanced SNR (figure 6).

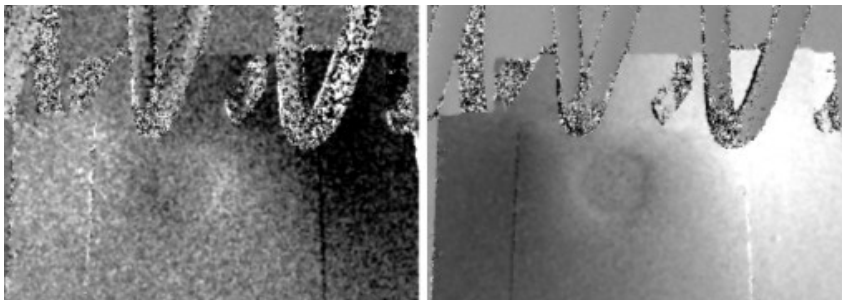

Figure 6: Insufficient bonding of PMMA to aluminium. Left: conventional shearography; right: Lockin phase image at 0.01Hz.

According to equation 1, the diffusion length of thermal waves depends on their frequency. Hence, the thickness of the layer that causes periodical buckling of an object due to thermal expansion can be adjusted. A series of measurements at various excitation frequencies was performed on an aluminium wedge embedded in epoxy (figure 7, left). The thickness of the epoxy covering the aluminium wedge increases continuously from 0mm to 3.3mm. As the diffusion length of the thermal waves increases with decreasing frequency, more and more of the wedge becomes visible (figure 7). The point of the phase reversal moves continuously downwards.

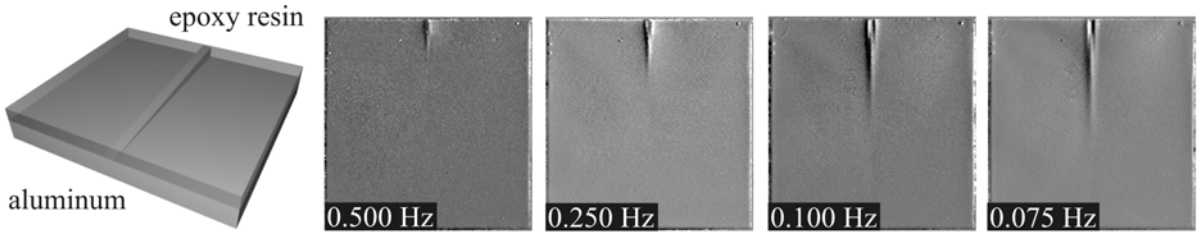

Figure 7: Optically excited Lockin shearography of aluminium wedge embedded in epoxy resin (left). Right: Phase images obtained at various modulation frequencies.

In figure 8, the phase angle at 0.075Hz along the dashed line is shown on the right as a function of thickness normalised to thermal diffusion length. This kind of curve is well known from surface monitoring of optically generated thermal waves where phase angle depth range is limited to about twice the thermal diffusion length [9]. However, depth range of Lockin Interferometry can be up to three thermal diffusion lengths since the thermal wave of the whole volume contributes to the signal [10].

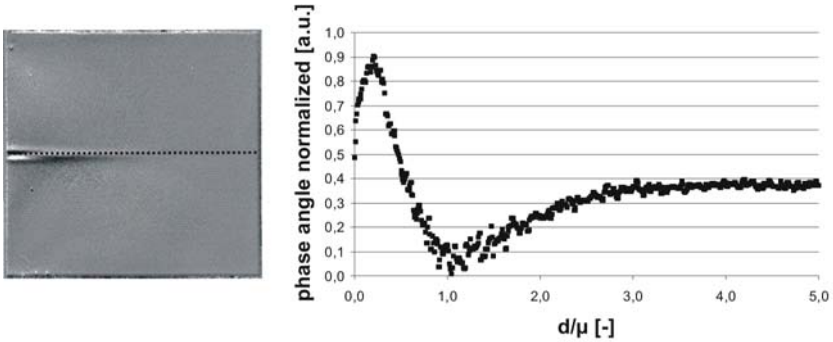

Figure 8: Phase image at 0.075Hz (left), phase angle taken along dashed line (right).

The influence of a variation of the modulation frequency of eddy current excitation is demonstrated in figure 9. The thermal wave is generated directly at the boundary of aluminium and adhesive. The insufficient bonding of PMMA to aluminium can only be detected if the range of the thermal wave exceeds the thickness of the PMMA plate. This depends directly on the Lockin frequency.

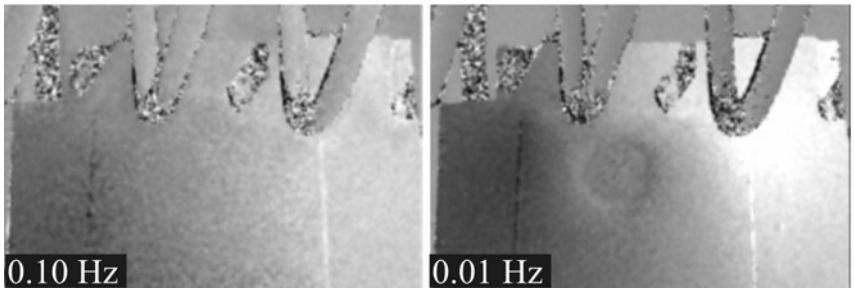

Figure 9: Lockin phase images of an insufficient bonding of PMMA to aluminium at two excitation frequencies: left 0.1Hz, right 0.01Hz.

In figure 10, two samples demonstrate a disbond between aluminium and GFRP or CFRP, respectively. In the GFRP/aluminium sample, the thermal wave is generated at the boundary of aluminium and adhesive. The disbond changes the local phase angle of the modulated object displacement and therefore clearly reveals the defect. In the CFRP/aluminium sample, not only the metal is heated, but the CFRP as well. Furthermore, CFRP is much stiffer than GFRP. The defect can still be observed, but not as clearly as under GFRP.

Figure 10: Lockin phase images at 0.01Hz of a disbond in combinations of a GFRP / aluminium (left) and CFRP / aluminium (right).

The results of comparative measurements of the sample with an insufficient bonding of PMMA to aluminium with conventional shearography and inductive and optical excitation, respectively, are shown in figure 11. The optical heating induces a high temperature gradient between the top and the bottom of the sample, causing a large displacement of the whole sample which hides the defect (figure 11, right). Inductive excitation, however, does not heat the surface, but the aluminium below. The displacement of the whole structure is reduced, and the defect can be detected due to the distorted heat transfer at the spot with the missing adhesive and therefore a different thermal expansion.

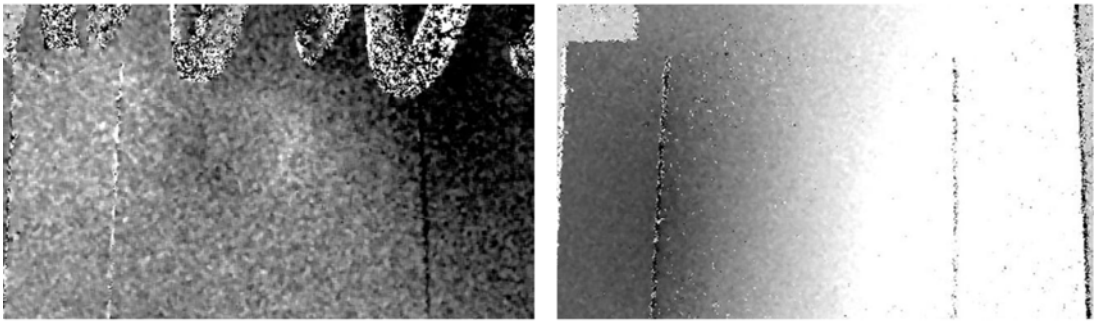

Figure 11: Insufficient bonding of PMMA to aluminium. Left: conventional shearography with inductive excitation; right: conventional shearography with optical excitation.

In figure 12, the same sample was measured with induction Lockin shearography and optically excited Lockin shearography. In both Lockin phase images the whole body displacement is reduced, but the defect is seen more clearly in the phase image obtained with modulated eddy-currant excitation. This accounts to the high damping of thermal waves. The interaction between the thermal wave generated by eddy current and the thermal boundary at the simulated defect is much higher because the thermal wave is generated right next to it. In the case of optical heating, the wave has to diffuse through 2mm of PMMA before it reaches the defect.

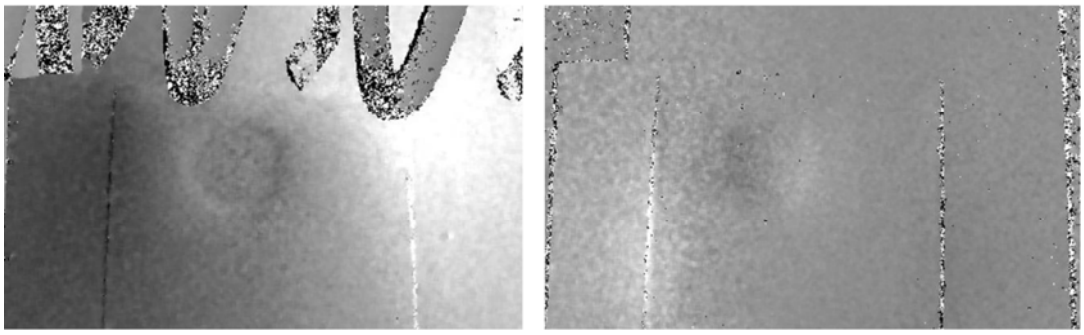

Figure 12: Insufficient bonding of PMMA to aluminium. Lockin phase image at 0.01Hz, measured with modulated inductive excitation (left) and modulated optical excitation (right).

Applications

The CFRP/foam-sandwich rims shown in figure 13 are in-service parts of a racing car which was built for the formula student team of the University of Stuttgart. These rims' weight is half the one of rims made from aluminium, but they are more sensitive to damage. Lockin shearography measurements revealed cracks in all torque arms, while conventional shearography failed due to a poor SNR and speckle decorrelation because of the need of a high load.

Figure 13: CFRP/foam rim made for formula student race car (left). Middle: conventional shearography result (poor SNR, high speckle decorrelation, only one fault detectable, see white mark). Right: Lockin phase image at 0.125 Hz (cracks in each torque arm, see white marks).

A CFRP tube with an impact damage was tested at an excitation frequency of 0.05Hz. The best image from the image stack (which complies with a conventional shearography measurement) reveals the defect, but there is a lot of noise (figure 14, left). In the Lockin phase angle image, the defect can be observed much more clearly (figure 14, right).

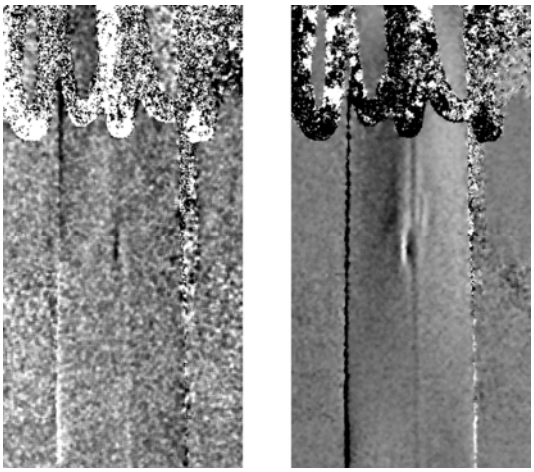

Figure 14: Eddy current-excited Lockin shearography: best image from image stack (left) and Lockin phase image at 0.05Hz (right).

A part of a CFRP landing flap with a stringer rupture was measured both with eddy-current excited Lockin shearography and optically excited Lockin shearography (figure 15).

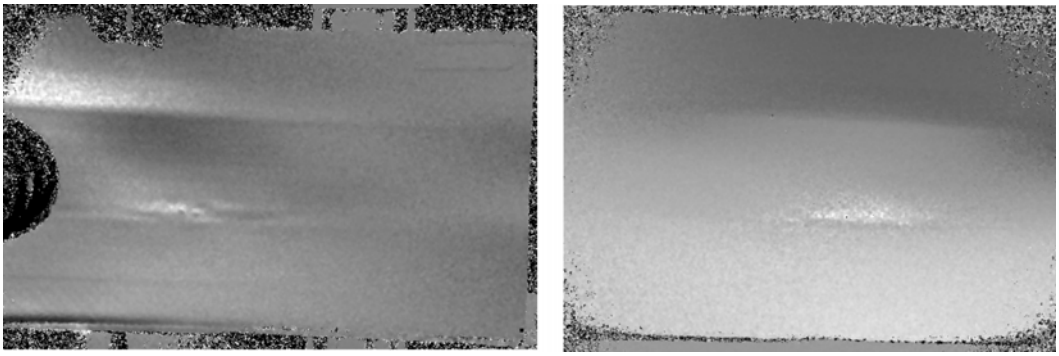

Figure 15: Lockin phase images of a CFRP structure at 0.01Hz measured with eddy current excited Lockin shearography (left) and optically excited Lockin shearography (right).

Modulated optical heating induces at the surface a thermal wave which diffuses into the material. At the stringer rupture, it is scattered and reflected, this way changing the local phase angle of the modulated object displacement. Inductive excitation, however, does not only heat the surface, but the whole structure. The whole body displacement of the structure is reduced (since the temperature gradient is much lower), and the defect is revealed much more clearly.

Summary
Conventional shearography is a fast and easy method for remote full field NDT. In combination with the Lockin technique, phase angle images are obtained, which show a reduction of whole body displacement effects and have an improved signal-/noise-ratio. This method is best applicable to polymer and composite structures due to their low thermal diffusivity and high thermal expansion. Modulated inductive heating is a new excitation technique for Lockin speckle-interferometry. Though there are some limitations concerning the sample geometry and the measurement field, the first results are very promising regarding some challenging problems in NDT which could not be solved by conventional speckle-interferometry so far. It is applicable for metals, metal/composite-combinations and CFRP.

Acknowledgements
The authors are grateful to the Institute of Aircraft Design (IFB) and the formula student race team (both University of Stuttgart) for kindly providing samples.

References
[1] J. A. Leendertz and J. N. Butters, “An image-shearing speckle-pattern interferometer for measuring bending moments”, Journal of Physics E: Scientific Instrument 6, pp. 1107-1110 (1973).
[2] G. Busse, German patent No. DE 4203272- C2, 1-3 (1992).
[3] P. K. Kuo, Z. J. Feng, T. Ahmed, L. D. Favro, R. L. Thomas and J. Hartikainen, “Parallel thermal wave imaging using a vector lock-in video technique”, Photoacoustic and Photothermal Phenomen, edited by P. Hess and J. Pelzl, Springer, Heidelberg (1987), pp. 415-418.
[4] D. Wu, “Lockin-Thermographie fuer die zerstoerungsfreie Werkstoffpruefung und Werkstoffcharakterisierung“, Ph.D. Thesis, University of Stuttgart (1996).
[5] H. Gerhard and G. Busse, “Use of ultrasound excitation and optical Lockin method for speckle interferometry deformation measurement”, in Nondestructive Characterisation of Materials XI, Springer-Verlag, Berlin (2003), pp. 525-534.
[6] H. Gerhard, “Entwicklung und Erprobung neuer dynamischer Speckle-Verfahren für die zerstoerungfreie Werkstoff- und Bauteilpruefung, Ph.D. Thesis, University of Stuttgart (2007), pp. 59-61.
[7] H. Gerhard, P. Menner and G. Busse, “Neue Möglichkeiten und Anwendungen der Lockin-Speckle-Interferometrie für die zerstoerungsfreie Pruefung, in Stuttgarter Kunststoff-Kolloquium 20, 5V3, Stuttgart (2007), pp.1-8.
[8] A. Rosencwaig and A. Gersho, “Theory of the photo-acoustic effect with solids”, Journal of Applied Physics 47, pp. 64-69 (1976).
[9] G. Busse, “Optoacoustic phase angle measurement for probing a metal”, Appl. Phys. Lett. 35, pp. 759-760 (1979).
[10] G. Busse and A. Rosencwaig, “Thermal wave piezoelectric and microphone detection for non-destructive evaluation: a comparison“, J. Photoacoustics 1, pp. 365-369 (1983).